Adaptive Tight Frames for X-ray CT Image Restoration via Radon Domain Inpainting

Bin Dong, Ruohan Zhan

December 12, 2015

Outline

Reviews and Preliminaries

X-ray CT Image Construction

- Collect attenuated X-ray data using a number of detectors with respect to different X-ray point sources and then to convert these detected data into an image.
- A serious clinical concern: additional imaging dose to patients' healthy radiosensitive cells or organs.
- Strategy: **sparse angular sampling**

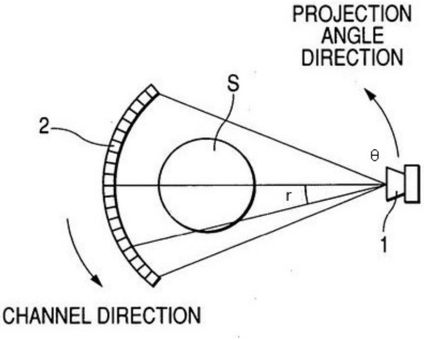

Figure 1: planer fan beam configuration : X-rays are constrained to be collimated to reduce the degradation caused by X-ray scattering.

$$P^{\theta,r}(u) = \int_0^{L^{\theta,r}} p(u(\mathbf{x}_\theta + \mathbf{n}l))\mathrm{d}l \quad \Rightarrow \quad f = Pu + \epsilon \tag{1}$$

where P is the projection operator, u is the image remained to be restored, f is the projected image and ϵ denotes the noise.

P is under-determined due to projection number decrease, thus direct methods like Filtered Backprojection(FBP), Pseudo Inverse Method(PIM) fail from full of artifacts and lack of stability.

Two Powerful Solvers: TV and Wavelets

Standard TV regulation:

$$\min_u \frac{1}{2}\|Pu - f\|_2^2 + \lambda\|\nabla u\|_p \tag{2}$$

Standard wavelets regulation:

$$\min_u \frac{1}{2}\|Pu - f\|_2^2 + \lambda\|Wu\|_p \tag{3}$$

Limitations: Optimize restored image u with the given primal projected image f or modified f, thus were not able to dig out more information when u is modified throughout the whole optimization.

A Joint Optimization Model over u and f

$$\begin{aligned}\min_{f,u} \quad & \frac{1}{2}\|R_{\Lambda^c}(Pu-f)\|_2^2+\lambda_1\|W_1 f\|_1+\lambda_2\|W_2 u\|_1+ \\ & \frac{\kappa}{2}\|R_\Lambda f-f_0\|_2^2+\frac{1}{2}\|R_\Lambda(Pu)-f_0\|_2^2\end{aligned} \tag{4}$$

which is solved efficiently via an alternative optimization algorithm[1].

Limitations: empirical regularized wavelet frames W_1, W_2 could not be optimal for special tasks.

Data-driven Tight Frames

Cai etc. in[2] proposed a variational model to learn adaptive tight frames from data itself:

$$\min_{v,W} \quad \lambda^2 \|v\|_0 + \frac{1}{2}\|Wu - v\|_2^2, \quad W^T W = I \tag{5}$$

which can be solved fast and stably via an alternative iteration algorithm.

Models and Algorithm

Model

$$\min_{f,u,v_1,W_1,v_2,W_2} \quad \frac{1}{2}\|R_{\Lambda^C}(Pu-f)\|_2^2+\frac{1}{2}\|R_\Lambda Pu-f_0\|_2^2+\frac{\kappa}{2}\|R_\Lambda f-f_0\|_2^2+ \\ \lambda_1\|v_1\|_0+\frac{\mu_1}{2}\|W_1 f-v_1\|_2^2+\lambda_2\|v_2\|_0+\frac{\mu_2}{2}\|W_2 u-v_2\|_2^2 \tag{6}$$

where R_{Λ^C} denotes the restriction on $\Omega \setminus \Lambda$, and R_Λ denotes the restriction on Λ.

Algorithms

Step Zero acquire u^0, f^0 via analysis wavelets model3.

Step One preconditioning W_1, W_2, v_1, v_2.

Step Two alternatively update $f, u, \{W_1, W_2\}, \{v_1, v_2\}$

(1) optimize f

$$\mathbf{f}^{k+1} \leftarrow \text{argmin}_f \frac{\kappa}{2}\|R_\Lambda f - f_0\|_2^2 + \frac{1}{2}\|R_{\Lambda^C}(Pu^k - f)\|_2^2 + \frac{\mu_1}{2}\|W_1^k f - v_1^k\|_2^2 + \frac{a}{2}\|f - f^k\|_2^2$$

(2) optimize u

$$\mathbf{u}^{k+1} \leftarrow \text{argmin}_u \frac{1}{2}\|R_{\Lambda^C}(Pu - f^{k+1})\|_2^2 + \frac{1}{2}\|R_\Lambda Pu - f_0\|_2^2 + \frac{\mu_2}{2}\|W_2^k u - v_2^k\|_2^2 + \frac{b}{2}\|u - u \tag{7}$$

(3) optimize W_1, W_2

$$\begin{aligned} \mathbf{W}_1^{k+1} &\leftarrow \mathrm{argmin}_{W_1} \frac{\mu_1}{2}\|W_1 f^{k+1} - v_1^k\|_2^2, \\ \mathbf{W}_2^{k+1} &\leftarrow \mathrm{argmin}_{W_2} \frac{\mu_2}{2}\|W_2 u^{k+1} - v_2^k\|_2^2 \end{aligned} \tag{8}$$

(4) optimize v_1, v_2

$$\begin{aligned} \mathbf{v}_1^{k+1} &\leftarrow \mathrm{argmin}_{v_1} \lambda_1\|v_1\|_0 + \frac{\mu_1}{2}\|W_1^{k+1} f^{k+1} - v_1\|_2^2, \\ \mathbf{v}_2^{k+1} &\leftarrow \mathrm{argmin}_{v_2} \lambda_2\|v_2\|_0 + \frac{\mu_2}{2}\|W_2^{k+1} u^{k+1} - v_2\|_2^2 \end{aligned} \tag{9}$$

- update f:

$$f^{k+1} = (R_{\Lambda^c} + \kappa R_\Lambda + (\mu_1 + a)I)^{-1}(R_{\Lambda^c} P u^k + \kappa R_\Lambda f_0 + \mu_1 {W_1^k}^T v_1^k + a f^k) \tag{10}$$

- update u:

$$u^{k+1} = (P^T P + (\mu_2 + b)I)^{-1}(P^T R_{\Lambda^c} f^{k+1} + P^T R_\Lambda f_0 + \mu_2 {W_2^k}^T {v_2}^k + b u^k) \tag{11}$$

- updating W_1, v_1 is almost the same as W_2, v_2.

  reformulate f, W_1, v_1 into F, V_1, D_1

$$\begin{cases} D_1^{k+1} = X_1 Y_1^T, \quad \text{where } X_1 \Sigma_1 Y_1^T = F^{k+1} (V_1^k)^T \\ V_1^{k+1} = \mathcal{T}_{\sqrt{\lambda_1/\mu_1}}((D_1^{k+1})^T F^{k+1}), \end{cases} \tag{12}$$

  see [2] for details

Convergence Analysis

we have proven that $\{u^k, f^k\}$ converges globally, and any sequence $\{u^k, f^k, v_1^k, W_1^k, v_2^k, W_2^k\}$ generated by proposed algorithm has subsequence convergence and the limit of every convergent subsequence is a stationary point of our model 6.

Lemma

The sequence $\{u^k, f^k\}$ is convergent globally, thus bounded.

Lemma

The sequence $X^k = (u^k, f^k, v_1^k, W_1^k, v_2^k, W_2^k)$ generated by Algorithms is bounded. For any convergent subsequence $X^{k'}$ with limit point $X^* = (u^*, f^*, v_1^*, W_1^*, v_2^*, W_2^*)$, we have

$$\lim_{k' \to \infty} f_1(v_1^{k'}) + f_2(v_2^{k'}) = f_1(v_1^*) + f_2(v_2^*) \tag{13}$$

and

$$\lim_{k' \to \infty} F(X^{k'}) = F(X^*) \tag{14}$$

Lemma

Denote $X^k := (u^k, f^k, v_1^k, W_1^k, v_2^k, W_2^k)$ as sequence generated by Algorithm and let Ω_* denote the set containing all limit points of X_k. Then Ω_* is not empty and

$$F(X^*) = \mathsf{inf}_k F(X^k), \quad \forall X^* \in \Omega_* \tag{15}$$

Theorem

The sequence $X^k := (u^k, f^k, v_1^k, W_1^k, v_2^k, W_2^k)$ has at least one convergent subsequence, and any limit point is a stationary point of model 6.

Numerical Experiments

It has been shown in [1] that wavelets based inpainting model4 has better performance than TV-based model and wavelet analysis model. Therefore, we only focus on comparing our proposed model 6 with wavelet frame based model4 proposed in [1], with the same initial value given by analysis model3. We will show that our model not only achieves **better image restoration**, but also **consumes less time for one iteration and has a faster speed of error decay in some cases**.

dataset !!!!								
NP	initial value		previous model[1]			adaptive model		
	err	corr	err	corr	time	err	corr	time
15	14.09	98.29	12.70	98.61	288.91	10.72	99.01	489.21
30	6.79	99.61	6.25	99.67	1186.54	5.37	99.75	915.95
45	5.20	99.77	4.70	99.81	1550.63	4.24	99.85	1232.22
60	4.16	99.85	3.89	99.87	319.29	3.61	99.89	1920.31

Table 1: Comparison of relative error(in percentage), correlation(in percentage) and running time(in seconds).

dataset NCAT phantom								
NP	initial value		previous model[1]			adaptive model		
	err	corr	err	corr	time	err	corr	time
60	9.55	99.35	5.00	99.82	239.47	4.39	99.86	749.05
75	9.02	99.42	4.61	99.85	296.71	4.00	99.88	955.03
90	8.81	99.45	4.21	99.87	303.98	3.73	99.90	1278.47

Table 2: Comparison of relative error(in percentage), correlation(in percentage) and running time(in seconds).

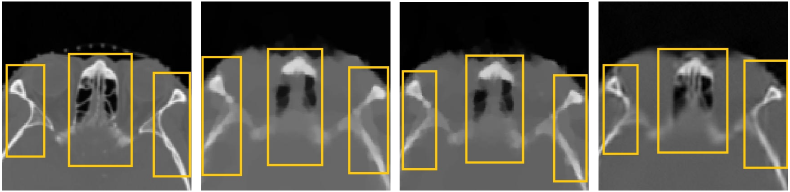

Figure 2: zoom-in patterns of dataset !!! for $N_P = 15$

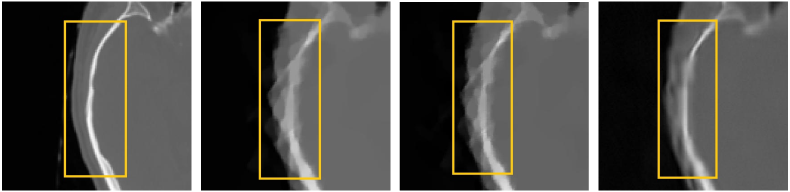

Figure 3: zoom-in patterns of dataset !!! for $N_P = 15$

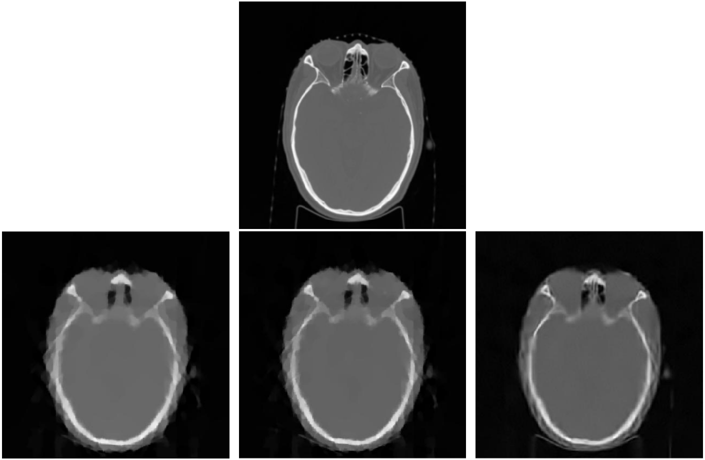

dataset !!!!				
N_P	15	30	45	60
adaptive model	0.51	1.12	1.87	2.35
wavelets model	0.95	1.76	2.53	3.32
NCAT phantom				
N_P	45	60	75	90
adaptive model	1.09	1.36	1.48	2.14
wavelets model	2.50	3.28	4.18	4.82

Table 3: Time(s) consumed of two models for one iteration on dataset !!!! and NCAT phantom.

Adaptive CT Image Construction

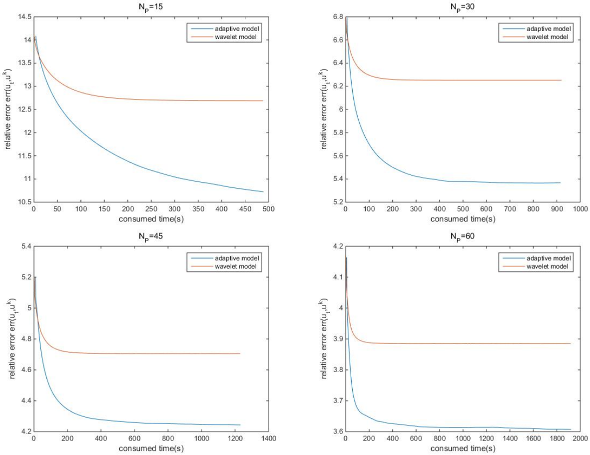

Figure 4: Relative error decreasing along with running time for !!!!

References

[1] Bin Dong, Jia Li, and Zuowei Shen. X-ray ct image reconstruction via wavelet frame based regularization and radon domain inpainting. *Journal of Scientific Computing*, 54(2-3):333–349, 2013.

[2] Jian Feng Cai, Hui Ji, Zuowei Shen, and Gui Bo Ye. Data-driven tight frame construction and image denoising. *Applied & Computational Harmonic Analysis*, 37(1):89ĺC105, 2014.

Questions?